A comparison of Eulerian and Lagrangian current measurements

Leo R. M. Maas

UDC 551.465.5

Summary

During three periods in 1981 and 1982, each lasting 3 to 4 days, Eulerian and Lagrangian currents were simultaneously observed at a moderate number of positions in the southern North Sea. These currents were divided into the ensemble averaged current, first order deformation terms and a turbulent part. The Eulerian and Lagrangian ensemble averaged current fields, except for the low-frequency part, compare well. Stokes' velocity estimates do not significantly improve on the mismatch of the residuals as the Eulerian shear is under sampled. The Eulerian shear matrix terms show a strong semi-diurnal spectral peak, whereas the Lagrangian spectrum is more or less flat as the drifters sample kinematically induced small-scale spatial velocity differences and therefore smear out this tidal peak. The turbulent fields yield estimates of the effective dispersion rates, which show that shear dispersion due to the tidal current is irrelevant at the time scales concerned. In agreement with the growth of a dye patch, released during one of the experiments, the drifter area grew very slowly or even decreased in time, indicative of anomalous dispersion. It is suggested that this may be due to the regularity of the bottom topography, as the generally highly nonlinear kinematic equations, describing the positions of particles in an idealized, tidally-varying Eulerian velocity field, then become (near-) integrable. In this view the (high) *normal* values of dispersion rates represent a coarse-grained parameterization of the chaotic processes, that arise from the nonlinearly coupled kinematic equations for a random bottom.

Ein Vergleich von Messungen Eulerscher und Lagrangescher Strömungen (Zusammenfassung)

Während dreier Meßkampagnen 1981 und 1982 von jeweils 3–4 Tagen wurden Eulersche und Lagrangesche Strömungen simultan an einer bestimmten Anzahl von Positionen in der südlichen Nordsee beobachtet. Diese Strömungen werden unterteilt in eine gemittelte Strömung, einen Deformationsterm erster Ordnung und einen turbulenten Anteil. Die gemittelten Eulerschen und Lagrangeschen Strömungsfelder sind in guter Übereinstimmung mit Ausnahme des niederfrequenten Anteils. Eine Abschätzung der Stokesschen Geschwindigkeit verbesserte nicht wesentlich die Diskrepanz zwischen den beiden Residuen, da die Eulersche Scherung nicht genau genug gemessen wurde. Die Terme der Eulerschen Scherungsmatrix zeigen einen starken halbtägigen Peak im Spektrum, während das Lagrangesche Spektrum mehr oder weniger flach ist, da die Drifter kinematisch induzierte, räumlich kleinskalige Geschwindigkeitsdifferenzen messen und deshalb den Gezeitenpeak verschmieren. Die turbulenten Felder ergeben eine Abschätzung der effektiven Dispersionsraten und zeigen, daß die Dispersion durch Scherung der Gezeitenströmung bei den betrachteten Zeitskalen von untergeordneter Bedeutung ist. In Übereinstimmung mit dem Anwachsen eines Farbflecks, der während des Experimentes ausgebracht wurde, wuchs das Drifterfeld sehr langsam bzw. nahm sogar mit der Zeit ab, was auf eine anormale Dispersion hindeutet. Es wird vermutet, daß dies mit der Regelmäßigkeit der Topographie zusammenhängt, da die allgemein hochgradig nichtlinearen kinematischen Gleichungen, die die Position von Teilchen in einem idealisierten, gezeitenabhängigen Eulerschen Geschwindigkeitsfeld beschreiben,

dann nahezu integrierbar werden. Unter diesem Gesichtspunkt repräsentieren die (hohen) normalen Werte der Dispersionsraten eine grobe Parametrisierung von chaotischen Prozessen, die aus den nichtlinearen gekoppelten kinematischen Gleichungen für eine zufällige Topographie entstehen.

Une comparaison des mesures eulériennes et lagrangienne de courants (Résumé)

Durant 3 périodes en 1981 à 1982, chacune durant de 3 à 4 jours, des courants eulériens et lagrangiens furent observés simultanément sur un nombre réduit de points dans le Sud de la Mer du Nord. Les courants furent décomposés en un courant moyen obtenu par une moyenne d'ensemble, des termes de déformation du premier ordre et une partie turbulente. Les champs de courants moyennés eulériens et lagrangiens sont comparables, sauf dans la partie basse-fréquence. Les estimateurs de vecteur vitesse de Stokes n'apportent pas d'améliorations significatives à l'erreur sur les résiduels lorsque le cisaillement eulérien est sous échantillonné. Les termes matriciels du cisaillement eulérien montrent un fort pic spectral semi-diurne, tandis que le spectre lagrangien est plus ou moins plat lorsque des échantillons de bouées dérivantes induisent de manière cinématique des différences spatiales à petite échelle de vecteur vitesse et donc gomment ce pic de marée. les champs turbulents permettent des estimations des taux de dispersion effective qui montrent que la dispersion de cisaillement due aux courants de marée n'a pas de signification pour les échelles de temps concernées. En accord avec la croissance d'une tache colorant, créée lors d'une des expériences, la zone de bouées dérivantes s'agrandit très lentement ou même se rétrécit, indiquant l'existence de dispersions anormales. Il est suggéré que cela soit dû à la régularité de la topographie du fond puisque les équations cinématiques, fortement non linéaires en général, décrivant la position des particules dans un champ idéalisé de vecteurs vitesse eulériens variant avec la marée, devient alors (presque) intégrable. Dans cette optique les valeurs "normales" (hautes) de taux de dispersion représentent une paramétrisation grossière des processus chaotiques que l'on obtient à partir des équations cinématiques couplées non linéairement pour un fond aléatoire.

1 Introduction

Back in the thirties Bjerknes, Bjerknes, Solberg and Bergeron [1933] remarked that if one is interested in general flow aspects of a hydrodynamic problem a consideration in the Eulerian frame is most appropriate. However, if one's interest is directed towards the evolution of some identifiable amount of material (fluid), a description in a Lagrangian framework, moving with the background flow, is demanded, such as in their case, where the evolution of cloud and weather systems was at focus. Remarkably, relatively few studies have been made from this viewpoint (exceptions are Pierson [1962], Attermeyer [1974], Sanderson [1985]) although many problems would require such a treatment, judging from the criterion by Bjerknes et al. [1933]. These problems range from such applied subjects as the spreading of fish larvae, or the spreading of solutes, to an intrinsically physical problem such as the evolution of eddies. This is presumably partly due to a lack of experience in dealing with the awkwardly nonlinear from which the dynamical laws of motion (and in particular the viscous terms, Monin [1962]) take in the Lagrangian framework. However, as was remarked by Sanderson [1985], this should not lead to prejudices, since the Eulerian equations, in full nonlinear form, are equally intractable. It is precisely the concept of linearisation which makes them amendable to analysis in both frames. Indeed a Lagrangian description may shed different light on a particular problem, as exemplified by Sanderson's [1985] study of the shape of internal waves, which, in the Lagrangian frame, takes on nonsinusoidal aspects in first order, such as encountered in a Eulerian description only in a second order treatment.

Another reason why a Lagrangian viewpoint is not frequently adopted may be the inherent difficulties in obtaining and interpreting Lagrangian observations. Whereas it is relatively easy to acquire Eulerian (current, temperature, pressure etc.) data from stand-alone mooring systems, drifting (Lagrangian) drogues have to be followed carefully and are sometimes difficult to recover once they start dispersing. Although satellites have now removed the problem of tracking, their interpretation is still problematic. Simultaneous Eulerian current measurements obtained at a set of I moorings (positions $\boldsymbol{x}^{(i)}$, $i = 1, \ldots, I$), can be viewed as yielding a sparsely, usually non-equidistantly sampled (at separation scales $L_{ik} = |\boldsymbol{x}^{(i)} - \boldsymbol{x}^{(k)}|$) wave-number spectrum (Riepma [1987]). In Fig. 1, such a hypothetical wave-number spectrum is plotted. More clearly than in theoretical or numerical formulations, this sparsely filled spectrum demonstrates the artificial way in which different physical processes are attributed to different parts of the wave-number domain. It is entirely dependent upon the observer's viewpoint (the separation scales L_{ik}), whether a phenomenon is regarded advection, being entirely deterministic (features with scales $\lambda > L_{\max} \equiv \max\{L_{ik}\}$), as turbulence, being entirely stochastic (features with scales $\lambda < L_{\min} \equiv \min\{L_{ik}\}$), or as shear dispersion, being of a mixed deterministic-stochastic type with scales $L_{\min} \leq \lambda \leq L_{\max}$. The difficulty now with Lagrangian data is that the spectral scales L_{ik}^{-1}, at which the wave-number spectrum is sampled are changing with time. This hampers their interpretation, as, for the typical situation where drifters disperse in time, their mutual distances (and in particular $L_{\min}$) increase and related wave numbers decrease. As a consequence, the turbulent part of the spectrum (the sub grid scale motions), i. e. the integral of the variance above $L_{\min}^{-1}$, increases, even if the eddies responsible for these motions are stationary.

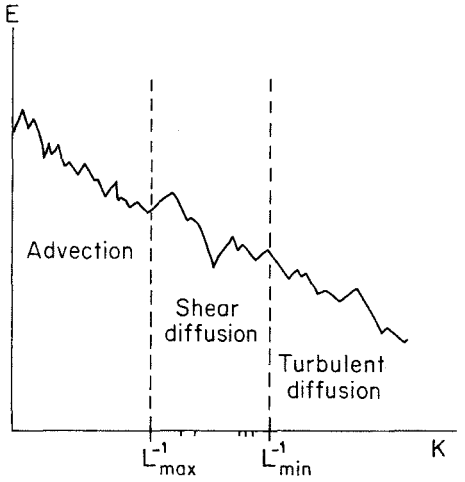

Fig. 1 Sketch of a possible wave-number spectrum. The tick marks at the horizontal axis are an example of a typical distribution of wave numbers at which observations are available. Given this configuration, the designation of different physical processes to different wave-number regimes is indicated.

A decomposition into a Fourier series (sinusoids) is not very feasible for a non-equidistant grid. As an alternative Molinari and Kirwan [1975] and Okubo and Ebbesmeyer [1976] propose a decomposition into a Taylor series (polynomials), where deformations at successive orders enter as Taylor series coefficients:

$$\boldsymbol{u}(\boldsymbol{x}^{(i)}) = \boldsymbol{u}(\bar{\boldsymbol{x}}) + (x_j^{(i)} - \bar{x}_j)\,\frac{\partial \boldsymbol{u}}{\partial x_j}(\bar{\boldsymbol{x}}) + (x_j^{(i)} - \bar{x}_j)\,(x_k^{(i)} - \bar{x}_k)\,\frac{\partial^2 \boldsymbol{u}}{\partial x_j\,\partial x_k}(\bar{\boldsymbol{x}}) + \boldsymbol{u}'(\boldsymbol{x}^{(i)}).$$

Here $\boldsymbol{u}(\boldsymbol{x}^{(i)})$ are observed 2D (Eulerian, or Lagrangian) currents at I positions $\boldsymbol{x}^{(i)}$ at time t, expanded about the centroid position $\bar{\boldsymbol{x}} = 1/I \sum_{i=1}^{I} \boldsymbol{x}^{(i)}$. Usually the number of current meters or drogues is so small that one is satisfied with the lowest order deformation terms: the mean $\bar{\boldsymbol{u}} \equiv \boldsymbol{u}(\bar{\boldsymbol{x}})$, the shear matrix (first order deformations)

$$\Omega = \begin{bmatrix} \bar{u}_x & \bar{v}_x \\ \bar{u}_y & \bar{v}_y \end{bmatrix}$$

(where $\bar{u}_x \equiv \partial u/\partial x$ $(\bar{\boldsymbol{x}})$ etc.) and the residual $\boldsymbol{u}'$, which can again be interpreted as reflecting the uniform advection, linear shear and turbulent part of the spectrum, respectively. Occassionally, with larger number of drifters or current meters higher order deformation terms can be calculated. Sanderson and Okubo [1986] calculated up to fifth order deformation terms, but concluded that, once the mean and the first order deformation field is subtracted, most of the displacement of their drifters was caused by scales of motion much smaller than the cluster size, yielding relatively low values of quadratic and higher order deformation fields.

Besides the tractability of the data in terms of a Taylor series, there are two other reasons for dividing our velocity field in this way. First, we can test observed values of the shear matrix terms (or rather their physically more meaningful combinations: vorticity $\equiv \bar{v}_x - \bar{u}_y$, divergence $\equiv \bar{u}_x + \bar{v}_y$, stretching deformation $\equiv \bar{u}_x - \bar{v}_y$ and shearing deformation $\equiv \bar{v}_x + \bar{u}_y$) against theoretically predicted values, as we can set up dynamical equations for each of these shear matrix components. The best-known of these is the vorticity equation, where tidal and (sub-tidal) rectified vorticity is created in regions where the bottom is sloping by the Coriolis and bottom-frictional torque ($\sim 1/H$, where H denotes water depth), as when the tidal flow is along- or (partially) cross-isobath respectively (Zimmerman [1978], Robinson [1983]). In a similar way it can be shown that each of the other shear matrix terms, equally result from an interaction of tidal flow and topography. Second, lateral shear in the residual, or tidal current in combination with a dispersion mechanism in the transversal direction can account for increased dispersion rates in the longitudinal direction and is believed to be responsible for observed increased dispersion rates such as is inferred from growth of dye patches (Zimmerman [1986]).

Thus in this paper the Taylor series approach is employed to compare Eulerian and Lagrangian current observations. After briefly describing the experiments (Section 2), the Eulerian and Lagrangian observations at each time step are split into a mean: the ensemble averaged Eulerian current, versus the motion of the centre of mass (Section 3), the shear matrix terms (section 4) and the turbulent part (Section 5). Section 6 gives a discussion of the phenomena observed.

2 Experiments

After pioneering work on the construction of a window-shade drogue minimizing the direct wind drag (Mulder [1982] and Mulder and Manuels [1982]) and a number of preliminary experiments lasting 1 to 2 tidal cycles each (Mulder and Manuels [1980]), three major experiments, lasting 5 to 7 tidal cycles, were conducted by them, which will be reported on here. These experiments, consisting of the simultaneous determination of the positions of 4 to 5 drifters and Eulerian current measurement at 6 to 14 moorings at positions in their direct neighborhood, were carried out in the southern part of the North Sea (Fig. 2a). From 2 to 6 July 1981 the experimental site was near the 'Bruine Bank' (Fig. 2b), which has a series of along-coastal banks, some 10 km long, they are a few kilometers wide and have a through-crest height difference of about 10 m, in an area whose average depth is approximately 28 m. The tidal 'ellipse' in this area (Fig. 3a) has its major axis (≈ 90 cm s^{-1}) in the along-coastal direction, aligned with the dominating bathymetric features. Observe that the cross-

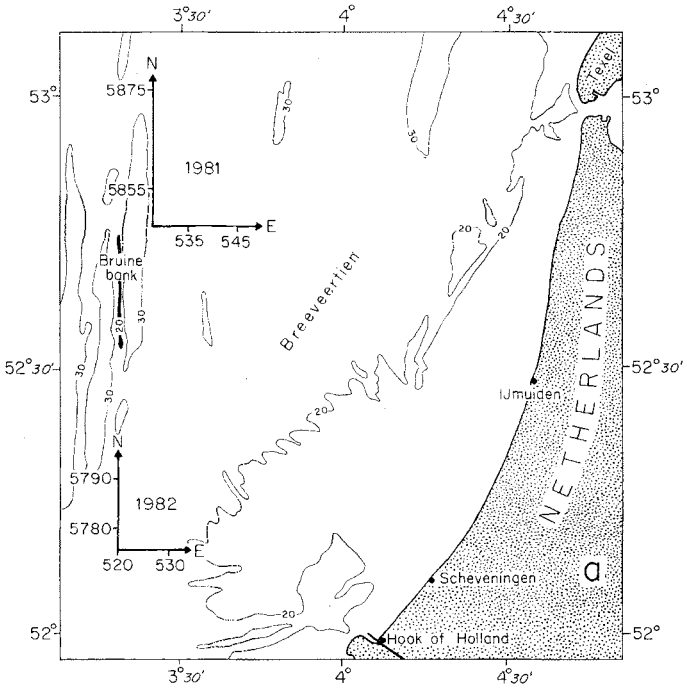

Fig. 2a Map of the southern part of the North Sea with the 'Bruine Bank' (1981) and 'Breeveertien' (1982) areas.

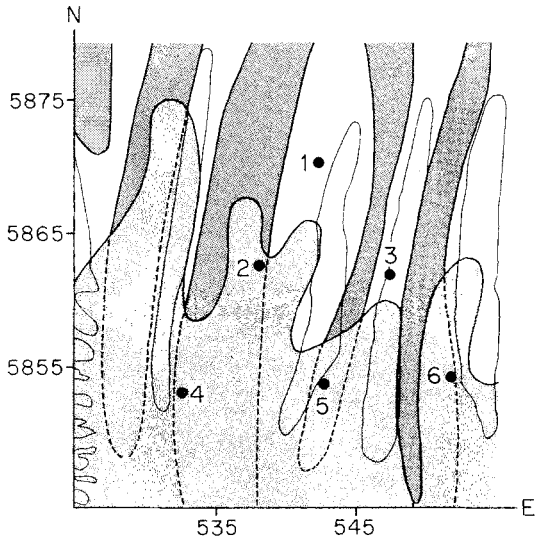

Fig. 2b Detail of 'Bruine Bank' morphology (from van Alphen and Damoiseaux [1987]), together with position of current meters (•), denoted by numerals, on a local UTM grid in km. Large-scale north-south oriented banks are enclosed by heavy solid / dashed lines, which reach (in the heavily shaded areas) up to 25 m. The 30 m isobath, also aligned in this direction, is given by the thin solid lines. The faintly shaded area in the south indicates the existence of meso-scale sand waves 2 to 4 m high.

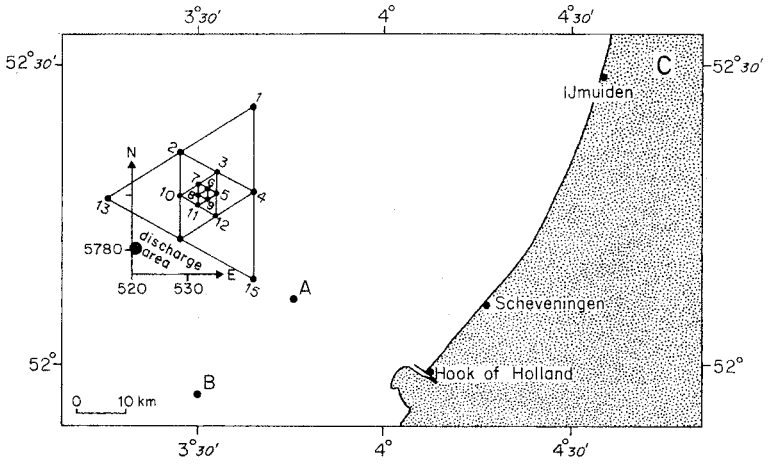

Fig. 2c 'Breeveertien' area with current meter mooring network (•) and discharge location of the dye (●) during the April 1982 period.

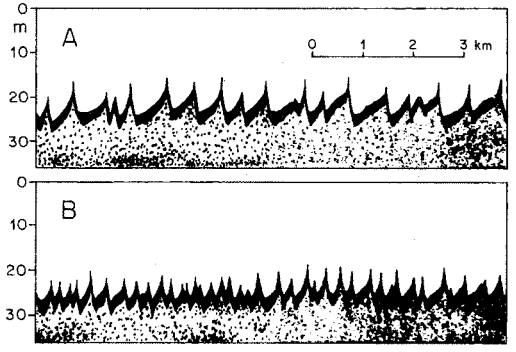

Fig. 2d Small-scale features at two positions labelled A and B in the 'Breeveertien' area, as observed by echo sounding equipment (from Dietrich and Ulrich [1967]).

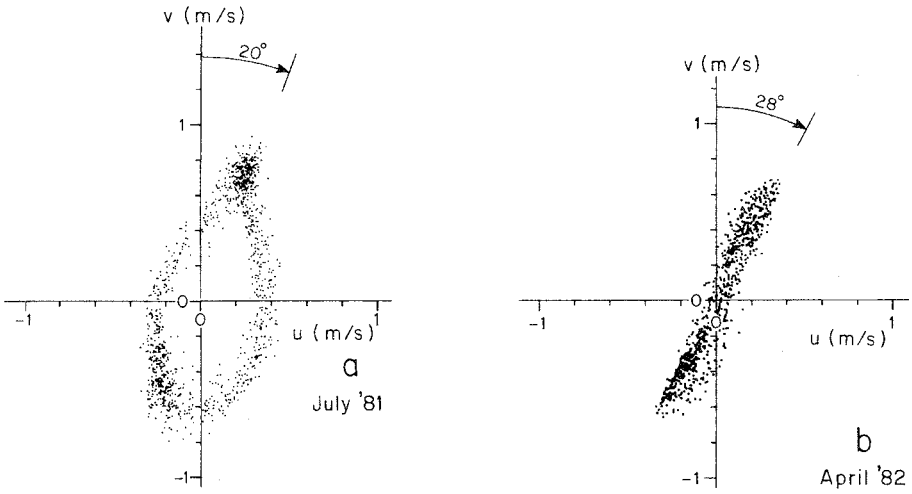

Fig. 3 Tidal 'ellipses' as observed by a single current meter in (a) 'Bruine Bank' and (b) 'Breeveertien' experiment.

isobath tidal flow of about 40 cm s^{-1} has an associated cross-isobath tidal excursion length scale (relevant to the response in the tide-topography interaction) which is similar to the width between the banks.

The other two experiments, carried out from 21 to 26 April and 10 to 13 May 1982, were performed in the 'Breeveertien' area (Fig. 2c). The bathymetry of this area is characterized by a series of sharp (wavelength ≈ 100 to 500 m) sand dunes with a through-crest height of approximately 10 m and length of about 1 km. They are *perpendicular* to the coast, superimposed on the gradual decrease of depth towards the coast (Fig. 2d). The overall average depth in this area is 23 m. The rectilinear tide of about 90 cm s^{-1}, Fig. 3b, is again in an along-coastal direction and thus perpendicular to the dunes. Remark that due to the small wave length and the orientation of the dunes the cross-isobath tidal excursion in these cases is much in excess of the topographic length scale.

The window-shade drogues were launched at mid-depth, they were 4 m wide and 4 to 7 m high. Their positions were determined every 6 seconds and subsequently averaged to 5 minutes on board of a ship by the Decca Hi-Fix 6 phase difference technique reported on in Mulder and Manuels [1982]. Positioning errors were less than 5 m. Due to malfunctioning, some of the drifters had to be serviced and relaunched during the experiments. Therefore positions (and each of their functionals) show data gaps and may change discontinuously. Current observations were performed in 1981 by Rijkswaterstaat at 10 minute intervals and in 1982 by the Royal Netherlands Meteorological Institute at 5 minute intervals at positions indicated in Figs. 2b and 2c, respectively.

3 The spatially averaged current

From subsequent positions of the drifters their velocity can be calculated, as well as their intermediate positions to which these apply. Averaging these velocities and intermediate positions over our ensemble of drifters we obtain the motion of the centre-of-mass. In Fig. 4 we have plotted the trajectory of our centre-of-mass for the 1981 experiment superimposed on the local bathymetry. As remarked, it reveals the strong alignment of banks and main tidal current direction, as well as the accurate fit of bank-width and cross-isobath tidal excursion scale. As we can infer from this trajectory, the tidal current ellipse is relatively open, in contrast to the ones obtained in the 1982 experiments (Fig. 5). The morphology in these experiments,

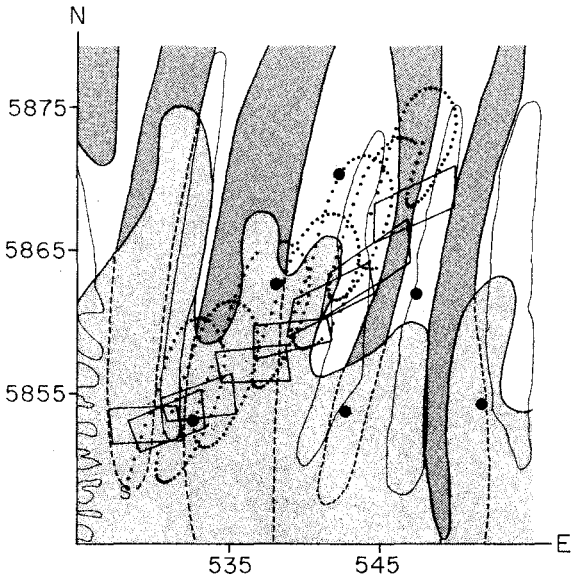

Fig. 4 The 'Bruine Bank' morphology, Fig. 2b, with trajectory of the centre-of-mass of the drifters (small dots) superimposed on it. The start position in this and subsequent figures is indicated by the letter S. Also shown is the configuration of the drifter area once every tidal cycle.

i.e. the sand dunes, are not shown in this figure as their scale is too small. The 'spaghetti' diagrams in Figs. 5c and 5d give the relative positions of the four drifters with respect to the centre-of-mass. The difference in 'behaviour' in April and May is due to a difference in separation-scales between the drifters (April: ≈ 2 km, May: ≈ 500 m) and will be discussed in the next section. In Fig. 6 the (tapered) Lagrangian current, obtained at the centre-of-mass, is compared for the April 1982 experiment to the ensemble averaged current of the 3 current meters closest to its trajectory. The Lagrangian and Eulerian currents compare relatively well. However, three principal differences are evident. First, the Eulerian current is about 15% weaker than its Lagrangian counterpart at the dominant semi-diurnal frequency. Second, there is a difference in the sub harmonic, diurnal frequency range (Fig. 7). Finally, there is a difference in the mean current, showing up most prominently in the net drift (Fig. 8).

Traditionally, differences between sub-tidal Lagrangian and Eulerian currents are related to the Stokes' velocity (Longuet-Higgins [1969]), a rectified current contribution due to a net correlation of tidally oscillating currents and their spatial gradients. In the original (theoretical) treatment these spatial variations are solely due to variations in the tidal phase, although Longuet-Higgins did advocate the use of triangular moorings (so-called Stokes' triangles), recognizing that in practical circumstances, spatial current variations are probably more due to local depth variations. This was experimentally confirmed (Ramster and Durance [1973]) and shaped in a model by Zimmerman [1979]. However, although in principal this offers a satisfying explanation of observed differences between Eulerian and Lagrangian currents, it does reveal the stringent need of Eulerian current information at a multiplicity of length scales; a need which is often not adequately met with in practice. This particularly applies to the 1982 experiments, where, as remarked, the dominant bathymetric features are sub-grid scale. This is the reason why Stokes' velocity estimates, whose calculations (using Zimmerman's [1979] scheme) are based on the observed Eulerian current shear are not matching with observed differences between Lagrangian and Eulerian currents (Mulder [1982]).

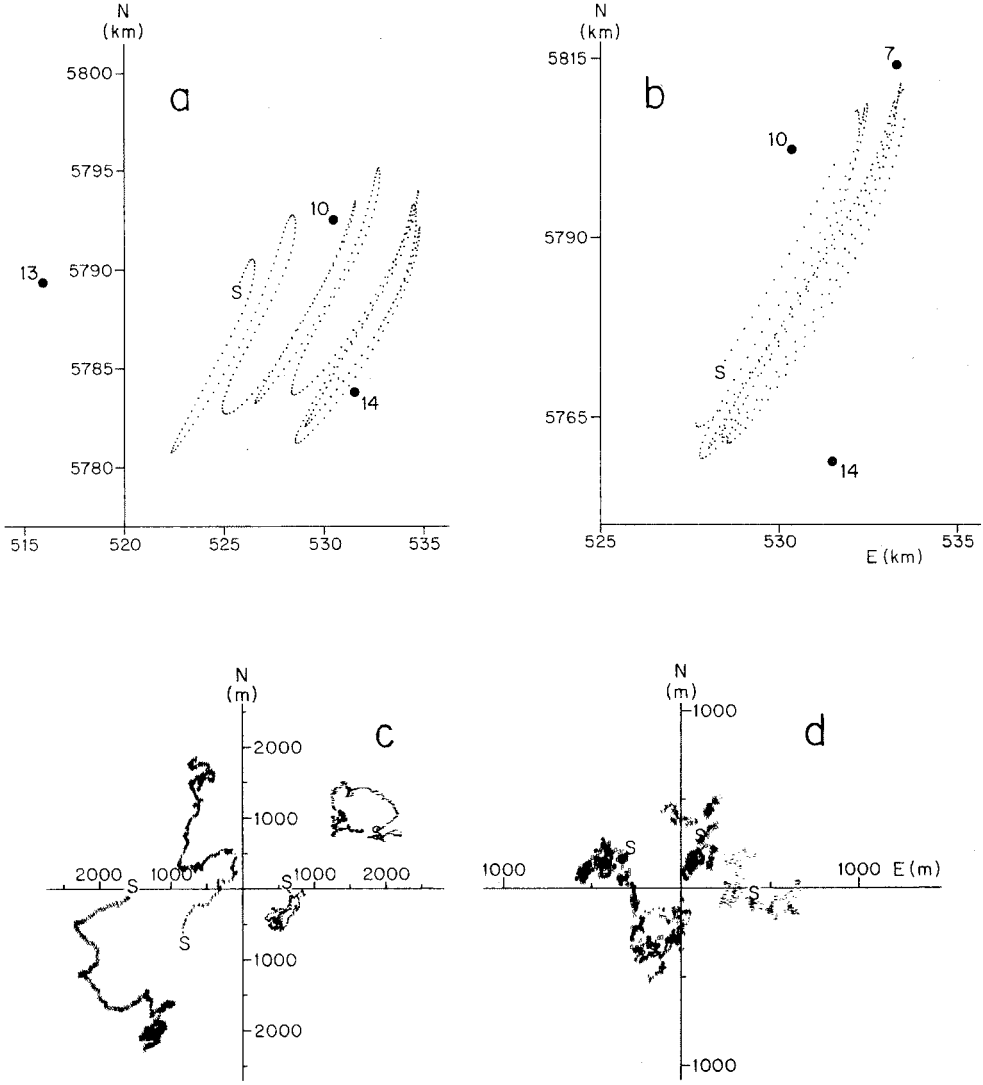

Fig. 5 Trajectories of centre-of-mass (Δt = 5 minutes) in (a) April and (b) May 1982. Locations of the three nearest current meters are indicated by numerals. Corresponding motions *relative* to the centre-of-mass is given in (c) April and (d) May.

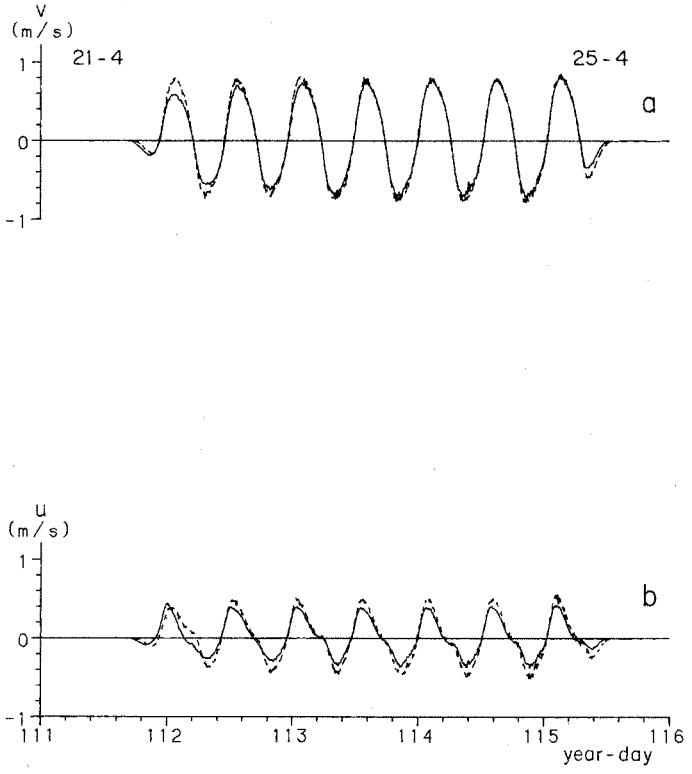

Fig. 6 Tapered Eulerian (solid lines) and Lagrangian (dashed lines) east (u) and north (v) velocity components. The Eulerian velocity is obtained as an average over the registrations by current meters 10, 13 and 14. The Lagrangian velocity is derived from the positions of the centre-of-mass of four drifters.

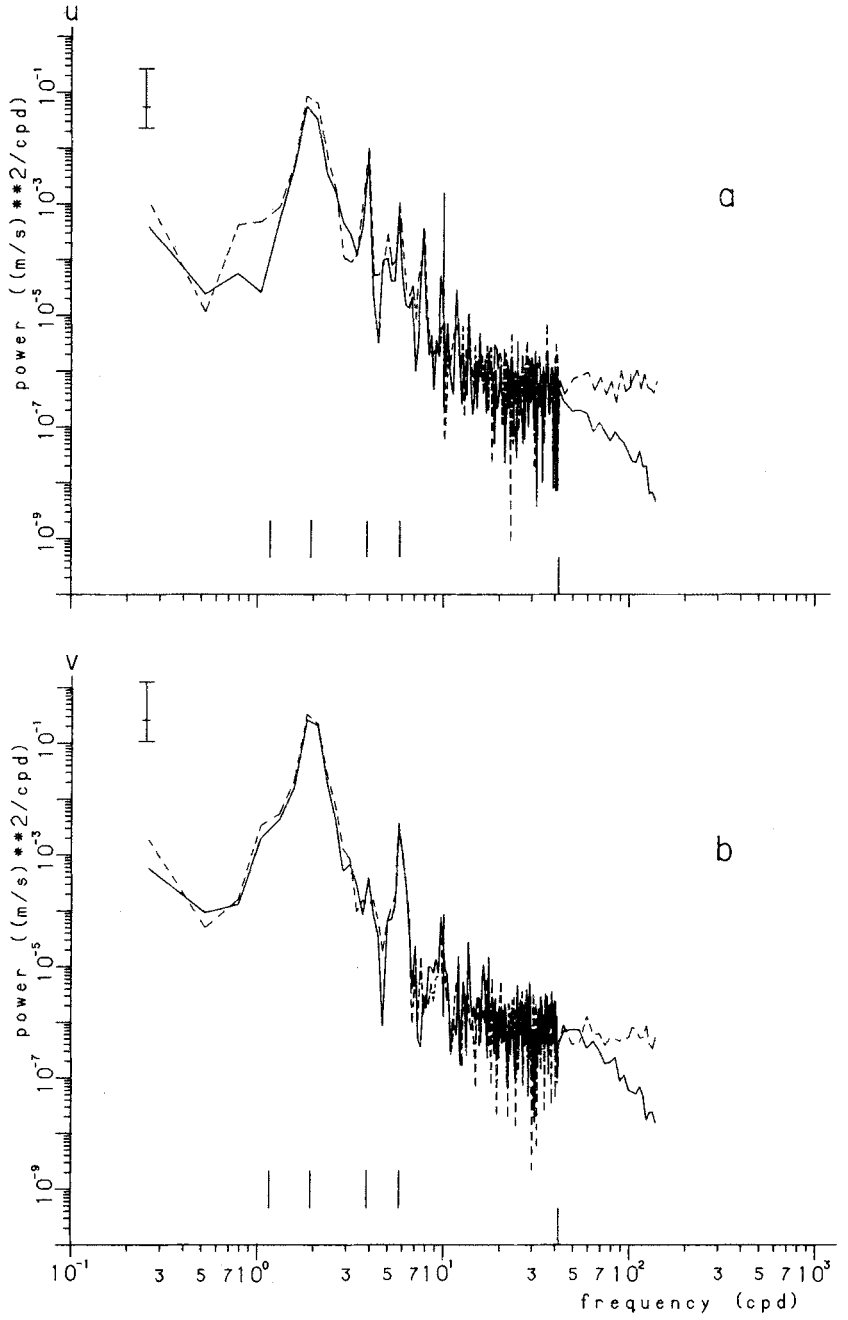

Fig. 7 Eulerian (—) and Lagrangian (- - -) power spectra of east (u) and north (v) components of velocity shown in Fig. 6.

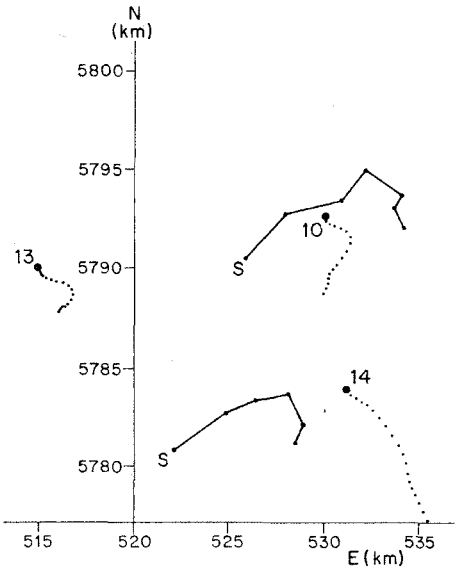

Fig. 8 Progressive vector diagrams of low-passed Eulerian currents at current meters 10, 13 and 14 (dotted curves) and subsequent Lagrangian positions of the centre-of-mass at two tidal phases (solid lines) for the period 21–25 April 1982.

4 The shear matrix

In the discussion of the Stokes' drift in the previous section the subject of the present section was inadvertently entered, revealing how much spectral current regimes are entangled. Time series of the four terms of the Lagrangian shear matrix, calculated by the method described in Okubo and Ebbesmeyer [1976], are given in Fig. 9a. They are rather *erratic*. For the April 1982 observations they are characterized by a strong decay in amplitude from the beginning of the measurements onwards. Since the configuration of the current meters, especially in 1982 (Fig. 2c), contain a large number of separation distances (from 2 to 32 km) we are able to calculate their Eulerian counterparts as a function of separation scale (Fig. 9b). This demonstrates the following features:

a) A much more pronounced (semi-diurnal) periodicity of each of the Eulerian shear matrix terms.
b) A correlation between *different* shear matrix terms for *similar* separation distances.
c) Phase jumps of 180° of the *same* shear matrix term over *different* separation distances.
d) A strong descrease in magnitude between the smallest scale (2 km) and larger scale separation distances, followed by a more gradual decay for still larger scales.

Aspects a, b and c indicate that, at least for the experiments in 1982, shear matrix terms are not *dynamically* generated, but are probably a manifestation of *kinematic* current shear, i.e., at this topographic length scale, $\lambda \leq 500$ m, velocity fluctuations are solely due to mass conservation:

$$\nabla \cdot (\boldsymbol{u}H) = 0,$$

from which,

$$\boldsymbol{u}H(\boldsymbol{x}) = \boldsymbol{Q}(t) + \hat{\boldsymbol{k}} \times \nabla \psi.$$

Here $H(\boldsymbol{x})$ denotes water depth, $\boldsymbol{Q}$ the time (t) varying barotropic (tidal plus residual) transport, $\hat{\boldsymbol{k}}$ is the vertical unit vector and ψ is a transport stream function, related to isolated eddies,

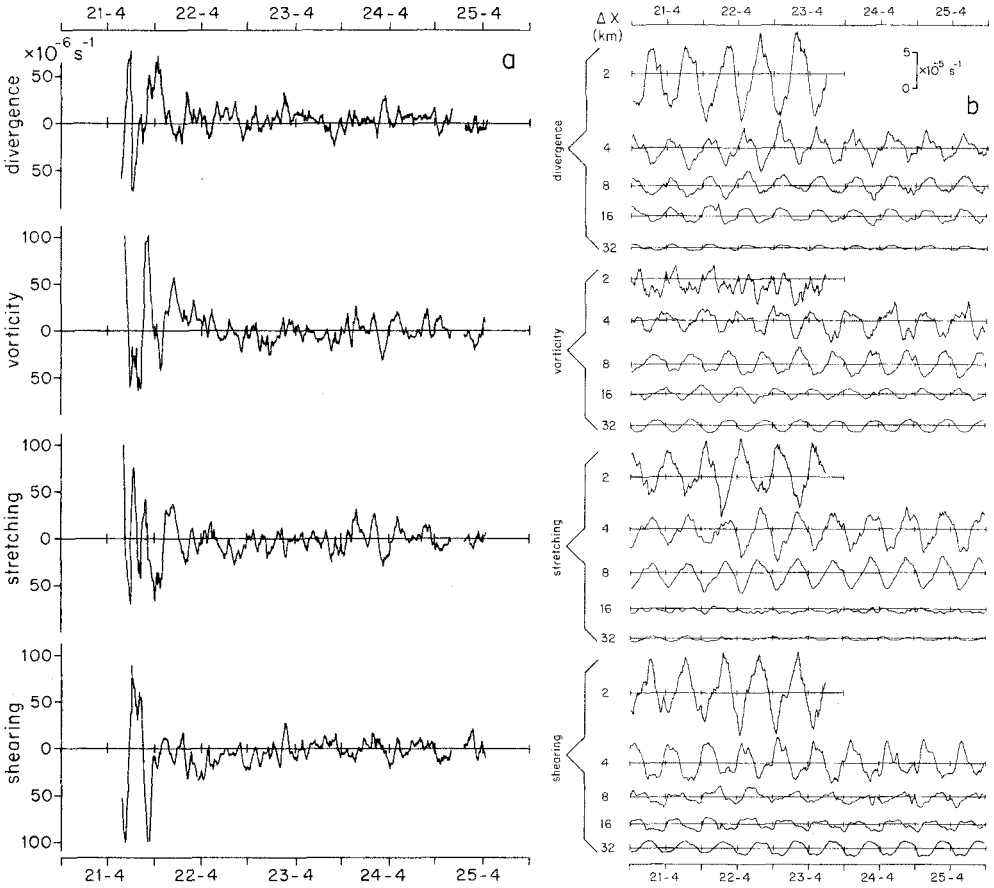

Fig. 9 Temporal development of divergence, vorticity, stretching and shearing deformation from the Lagrangian (a) and Eulerian (b, at different separation scales Δx) current measurements for the period 21–25 April 1982.

presently assumed small in comparison with the barotropic transport. Depth variations over the mooring positions are reflected in variations of the tidal (and residual) current amplitudes, this difference being fixed in time for fixed mooring positions. Drifters, however, travelling through such a spatially varying Eulerian current field, *sample* local depth fluctuations and, accordingly, their path acquires a much more erratic pattern. Finally it is easy to conceive of an arrangement of moorings in which depth differences between two adjacent pairs of moorings change signs, thus provoking a phase difference of 180° in the shear matrix terms as observed.

The strong scale dependence (aspect d), noted by R i e p m a [1987] for this data set and by e.g. K a w a i [1985] on an oceanic scale, can be taken as an experimental fact from which it would be evident that drifters, which by dispersion tend to increase their mutual distances, sample this Eulerian drop in amplitude of shear matrix terms, as in Fig. 9a. In order to *comprehend* this scale dependence itself, we may speculate that it can, on the one hand, be an artefact due to undersampling of kinematic current shear as the latter is organized at the topografic length scale (100 to 500 m) *aliased* to larger length scales (of which the 2 km separation distance is closest and accordingly acquires the largest magnitudes of the shear matrix components). On the other hand, it may be a manifestation of *horizontal shear dispersion*, a truly dynamical phenomenon. Horizontal shear, in combination with dispersion in a perpendi-

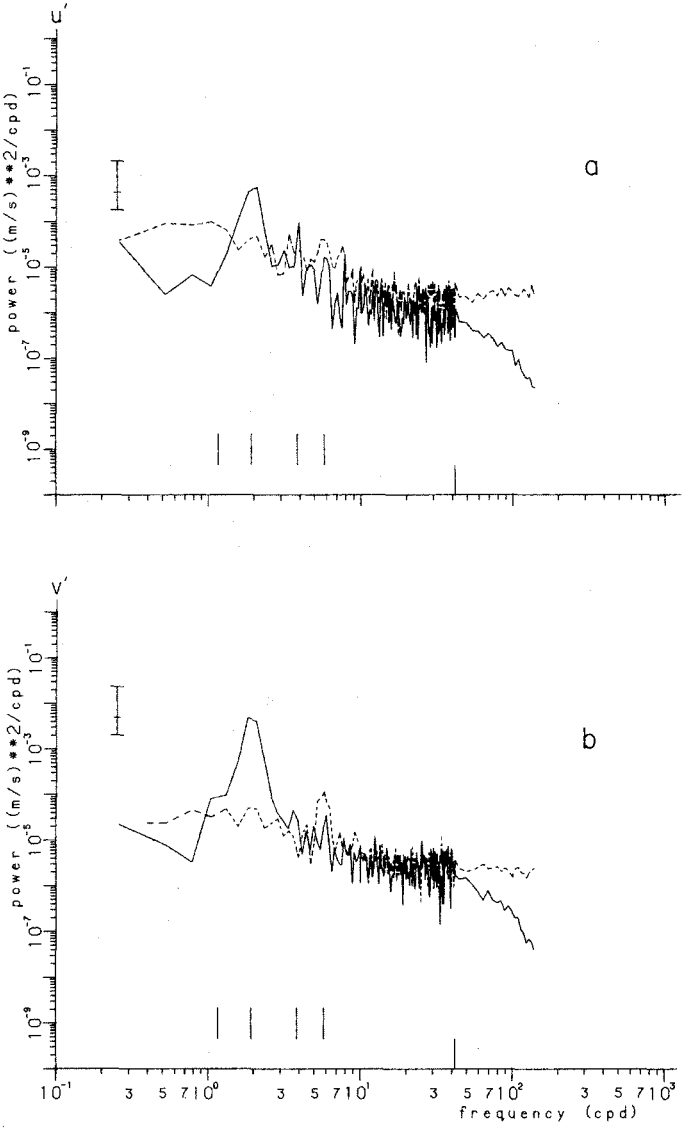

Fig. 10 Power spectra of the ensemble average of relative currents $u^{(i)} - \bar{u}$ for the east (u') and north (v') components for the April 1982 period. The Eulerian average (—) is based on the relative currents from moorings 10, 13 and 14; the Lagrangian (- - -) on the relative currents of the four drifters.

colar direction increases the dispersion in the direction of the tidal current and will yield a dispersion parameter $K \sim l^{4/3}$ (where l denotes length scale) in this context discussed by Zimmerman [1986]. Assume that the eddies responsible for the dispersion are in one of the spectral inertial sub ranges in between spectrally-localized energy inputs (Ozmidov [1965]), which thus feed their energy, E, at a constant rate to adjacent wave numbers ($dE/dt = \varepsilon$ = constant). A dimensional analysis, then, with velocity and length scales v and l, shows that $v^3/l = \varepsilon$ and thus a typical shear term $\Omega = v/l$ would yield $\Omega \sim l^{-2/3}$. This cascade of eddy-energy then represents a genuine decay of shear intensity with increasing length scale.

Fig. 10 shows east and north components of power spectra of relative currents (i.e. $\boldsymbol{u}^{(i)} - \bar{\boldsymbol{u}}$) from the April 1982 experiment averaged over

1) the nearest three current meters (numbered 10, 13 and 14, see Fig. 2c) and
2) the four drifters.

Their difference again reflects the conclusions arrived at before: Lagrangian current shear is a smeared-out version of Eulerian current shear (here distinctly visible as a strong albeit widened semi-diurnal peak, whereas the Lagrangian current spectrum is almost white).

Spectral smearing in a simple analytical model

There is one analytical example which offers a ready demonstration of this spectral smearing. Consider the nonlinear 1D kinematical relation

$$\frac{dx}{dt} = u_E\,(x,t),$$

where the Eulerian velocity, $u_E = Q(t)/H(x)$, which, at *fixed* x, is a simple harmonic function of time. Consider the nondimensional topography, $H(x)$, to be sinusoidally perturbed: $H(x) = 1 - \varepsilon \cos x$ ($\varepsilon < 1$), and the transport, Q, to consist of a residual and a tidal component: $Q = Q_0 + Q_1 \cos t$. Then the position of a water parcel, x, as a function of time, t, is determined by the relation

$$x - \varepsilon \sin x = Q_0\, t + Q_1 \sin t + \xi,$$

where ξ is the position of the parcel at time zero: $x(0) = \xi$. The inversion problem, obtaining x as a function of t, is, curiously, just Kepler's classic problem, who studied this equation in describing planetary motions (Watson [1966] § 17.2). Its solution is given by

$$x(t) = Q_0 t + Q_1 \sin t + \xi + \mathbf{Im}\left[\sum_{n=-\infty}^{\infty} \sum_{m=-\infty}^{\infty} J_n(n\varepsilon)\, J_m\,(nQ_1)\, \exp\,\{i(nQ_0 + m)\, t + in\xi\}\right],$$

where J_n is an n^{th} order Bessel function of the first kind and **Re**[...] and **Im**[...] denote the real and imaginary parts of the quantity in square brackets respectively. From this expression the Lagrangian velocity field is obtained as

$$u_L = \frac{\partial x}{\partial t} = Q_0 + Q_1 \cos t + \mathbf{Re}\left[\sum_{n=-\infty}^{\infty} \sum_{m=-\infty}^{\infty} (nQ_0 + m)\, J_n\,(n\varepsilon)\, J_m\,(nQ_1)\, \exp\,\{i(nQ_0 + m)\, t + in\xi\}\right]$$

This has a power spectrum which is filled with harmonics, in sharp contrast with the single-frequency spectrum of the Eulerian current we started out with.

Time series of the Lagrangian shear matrix terms for the 1981 experiment are much less erratic than the ones shown in Fig. 9a, reflecting a substantial *dynamically* generated part as the near-unity of the ratio of topographic length scale to cross-isobath excursion scale implies.

5 The turbulent field

Subtracting the centre-of-mass current, as well as the currents related to the linear shear, from the originally observed currents yields the 'turbulent' velocity contribution, $\boldsymbol{u}'$, organized at a sub-grid scale. In Fig. 11 we show a scatter plot of the turbulent velocity field of a single drifter, which exemplifies the stochastic nature of this field and suggests that it is Gaussian. In fact, a calculation of this turbulence intensity (the variance), averaged over the four drifters, shows a slight predominance of the turbulent velocities in the along-coastal (tidal) direction over its perpendicular component.

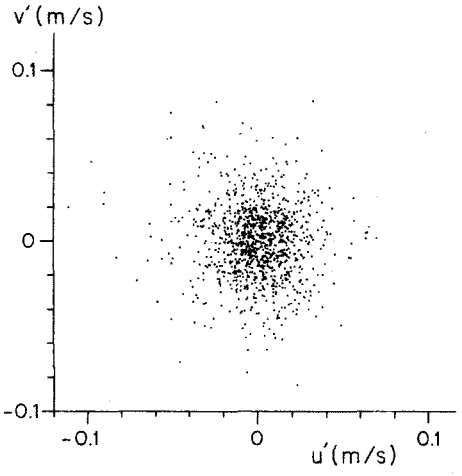

Fig. 11 Scatter plot of turbulent velocity of drifter 1 for July 1981, i.e. $\boldsymbol{u}'(\boldsymbol{x}^{(1)}) = \boldsymbol{u}(\boldsymbol{x}^{(1)}) - \{\boldsymbol{u}(\bar{\boldsymbol{x}}) + (\boldsymbol{x}^{(1)} - \bar{\boldsymbol{x}}) \cdot \nabla \boldsymbol{u}(\bar{\boldsymbol{x}})\}$.

As Okubo and Ebbesmeyer [1976] showed, a knowledge of the turbulent velocity and position fields allows a determination of the eddy-diffusion tensor (e.g. $D_{xx} = 0.1\,\overline{\sigma_x \sigma_{u'}}$, where σ_x and $\sigma_{u'}$ refer to the standard deviation of the 'turbulent' positions and velocities respectively and the bar indicates a tidally-averaged value). This, together with the magnitude of the shear matrix terms discussed in the previous section, allows an estimation of the magnitude of the *effective* dispersion coefficient in the longitudinal direction relative to the longitudinal dispersion rate proper.

As first discussed by Taylor [1953], increased effective longitudinal dispersion rates result due to a combination of shear of the dominant current component in its transverse direction in conjunction with a transversal turbulent mixing process. Remarkably, if the flow, u_0, (and therefore its shear) is *confined* in the transverse direction (as e.g. in a flow through a pipe, or in a flow with a sinusoidal, transversal variation) the effective longitudinal dispersion coefficient is *inversely* proportional to the transverse mixing coefficient D_{yy}, where from now on we associate x and y with the longitudinal and transverse directions, respectively. In an *unbounded* shear flow, however, the dispersion proceeds at an increased rate (the area-averaged variance $\sigma^2 \approx t^3$) such that the validity of the concept of a diffusion 'constant' (defined as $\frac{1}{2}\,\mathrm{d}\sigma^2/\mathrm{d}t$) is at stake. An oscillatory (period T) flow component, u_1, ensures an additional amount of mixing (Okubo's [1967] model applied in the horizontal plane, as advocated by Zimmerman [1986]) and leads to an effective dispersion coefficient *directly* proportional to the transverse mixing coefficient.

Young, Rhines and Garrett [1982] show how the effective dispersion coeffcient, K_{xx}, depends on the ratio $\tau = 2\pi TD_{yy}/L^2$ (L denoting the transversal wave length) of tidal period and cross-current mixing time-scale:

$$K_{xx} = D_{xx} + \frac{u_1^2 T}{8\pi}\left[\frac{\tau}{1+\tau^2}\right],$$

which reaches a maximum for $\tau = 1$. In the two limits 1) $\tau \to 0$, as when $L \to \infty$ (the unbounded oscillatory shear flow) and 2) $\tau \to \infty$, as when $T \to \infty$ (a steady 'confined' flow), the effective dispersion coefficient is again *directly* (Okubo [1967]), or *inversely* (Taylor [1953]) proportional to the transverse coefficient D_{yy} respectively. When, for horizontally unbounded shear flows, a residual and an oscillatory flow component are present simultaneously the dispersion due to the residual flow takes over at the increased rate ($\sigma^2 \approx t^3$) when

$$t > \frac{\sqrt{3}}{2\pi}\left[\frac{u_0 L_1}{u_1 L_0}\right] T \qquad (1)$$

(Okubo [1967]), L_0 and L_1 now referring to the transversal wave length of the residual and tidally varying components respectively. For sinusoidal flows it depends on the inverse nondimensional transversal mixing time-scale, τ, whether mixing by shear-dispersion due to the oscillatory current contributes as much to mixing as does the steady flow.

The observations provide us with linear shear matrix terms, thus yielding estimates of the unbounded shear flow only. As the approximation of a linearly increasing flow eventually breaks down, a consideration of bounded (sinusoidal) shear flows, as given above, is relevant.

Experimental diffusion estimates

The April 1982 observations yield the following estimates:

$$\frac{\partial u_0}{\partial y} = -10^{-7}\ \mathrm{s}^{-1}, \quad \frac{\partial u_1}{\partial y} = 8.10^{-6}\ \mathrm{s}^{-1}, \quad D_{xx} = 3\ \mathrm{m^2 s^{-1}}, \quad D_{yy} = 1\ \mathrm{m^2 s^{-1}}.$$

From these we find that the effective dispersion coefficient is approximately unaltered, $K_{xx} \approx D_{xx}$. This is because the transversal mixing time-scale $\tau << 1$, since the transversal length scale, L_1 (estimated from $\partial u_1/\partial y$, with $\Delta u_1 \approx 0.1\ u_1$), is relatively large ($\approx$ 10 km). Shear dispersion by the tidal current is thus unimportant. Of course, as discussed above, after sufficient time, when scales are of the order of L_0, residual shear dispersion will become important yielding dispersion at an increased rate.

During the April period a dye-release experiment was carried out simultaneously (see discharge location in Fig. 2c), which offered independent information on dispersion rates, described by Suijlen et al. [1990]. Fig. 12a compares concentration contours for a number of subsequent moments, with the enclosed drifter area. In Fig. 12b the increase of patch size as a function of time on a logarithmic scale is given over the complete time span that the dye could be traced. It reveals the existence of three separate regimes.

The first, from the time of release up to 25 hours, is characterized by a fast increase of patch size at a rate α, where $\sigma^2 \approx t^{\alpha}$, which fluctuates between $1 \leq \alpha \leq 3$, but has an average value of about 2. Fluctuations in the initial state are due to a more complicated time dependence of the variance (Okubo [1967]). Also, different realizations of dye-release may lead to different initial time behaviour, as the time of discharge within the tidal cycle is of relevance (Kalkwijk [1986]). However, after this initially rapid growth (up to a scale of about 4 km) a second linear ($\alpha = 1$) regime is expected, as the dye has then been mixed vertically and will be spreading horizontally due to genuine dispersion and shear-dispersion by the oscillatory current. The patch size observations indicate a reduced dispersion rate between 25 and 250 hours after release, which is, remarkably, at a much smaller rate $\alpha \approx 0.25$. To this period the

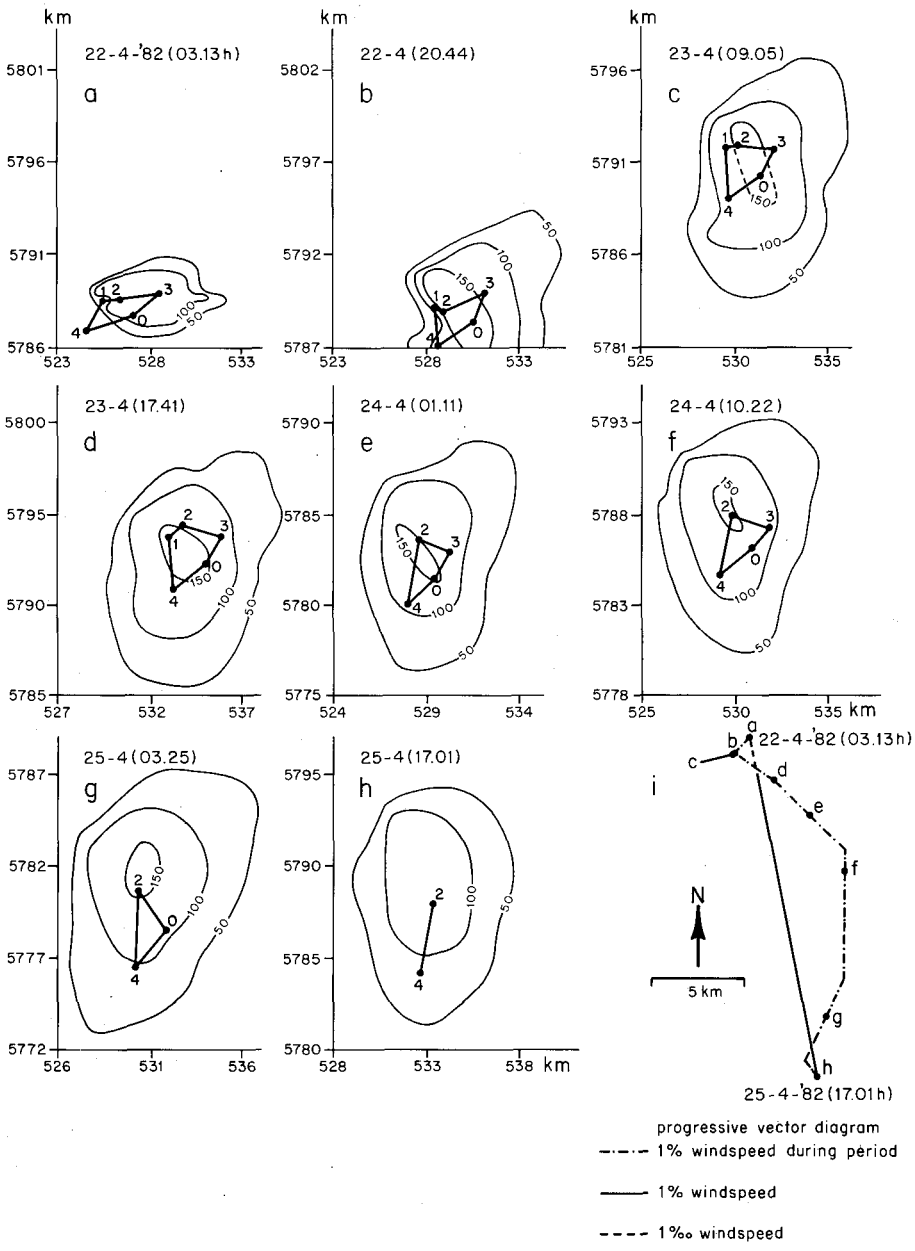

Fig. 12a Successive dye distributions (solid lines denote concentration contours) for the April 1982 experiment, together with the drifter configuration (labelled 0 through 4). The last panel shows the progressive vector diagram of the wind during each of the separate panels, as well as over the total period (from S u i j l e n et al. [1990]).

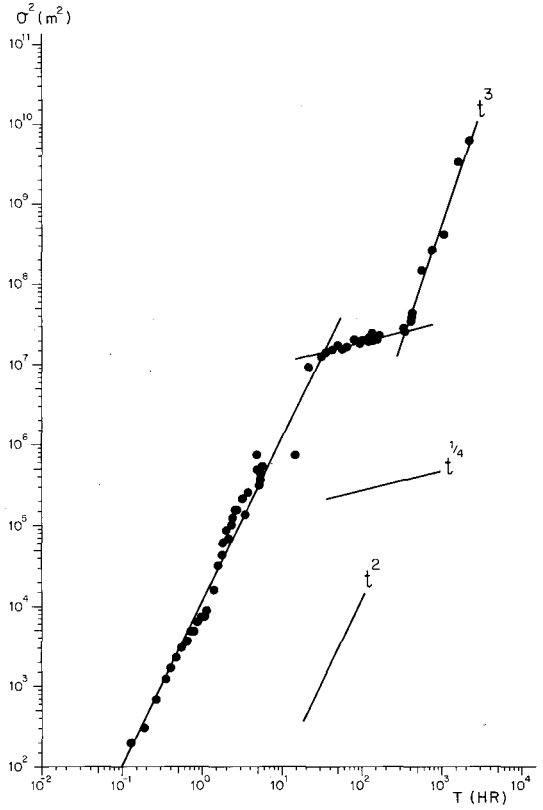

Fig. 12b Evolution of patch size of dye (where $\sigma^2 = 2\sigma_x\ \sigma_y$) during the April 1982 experiment (from Suijlen et al. [1990]).

drifters pertain. As they start off at a finite distance they should be treated as having a virtual starting point prior to the moment of launching. Curiously, the drifters also exhibit an increase at a rate ($\alpha \approx 0.7$) below the theoretically expected value $\alpha = 1$. After about 250 hours (at a scale of about 6 km) the dye patch size starts growing fast ($\alpha = 3$). Apparently the dispersion is then produced by shear-dispersion due to the residual current. The time needed for this transition to occur (twenty semi-diurnal tidal periods) corresponds to the time which (1) would give, using the observed values of the residual and semi-diurnal matrix magnitudes as given at the beginning of this section. Alternatively, assuming that tidal and residual shear are *both* induced by the topography and therefore have similar length scales ($L_0 = L_1$), then, with $u_1 = 90$ cm s^{-1} and $u_0 = 1.2$ cm s^{-1}, a transition at $t/T \cong 21$ is 'predicted'. Of course, there is uncertainty about the value of the residual current, which gives an equal amount of uncertainty in the estimated time of transition of the different dispersion regimes, but the observed transition time span is not inconsistent with this estimate.

Trapping

Anomalously reduced dispersion rates of the drifters are inferred by plotting the time evolution of the drifter area (Fig. 13a). This is even more substantiated when we plot the corresponding evolution in the other two experiments (Figs. 13b and c), where the drifter area is observed to *decrease* in time over a prolonged time span (several tidal periods), indicative

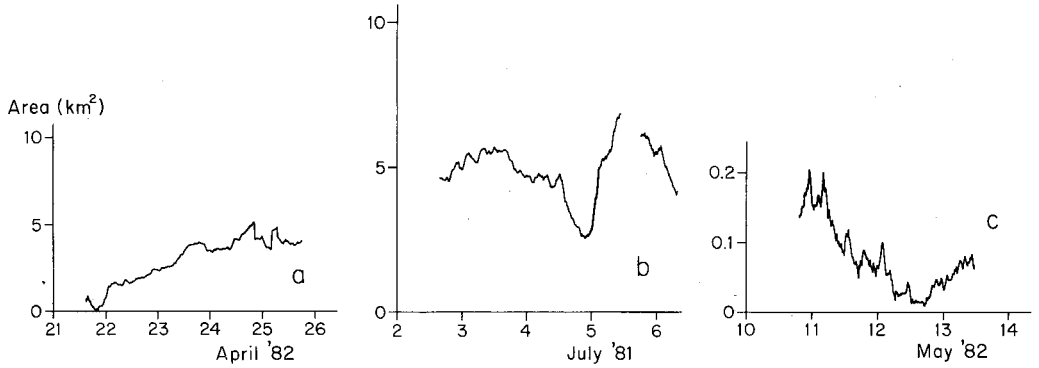

Fig. 13 Evolution of area enclosed by drifters (in km^2) for the April 1982 (a), July 1981 (b) and May 1982 (c) experiments.

of some *trapping* mechanism. A similar decrease in patch size has been observed over short periods (less than a tidal cycle) in other circumstances: by Kawai [1985] in a converging rip current, and Okubo et al. [1976], who related convergencies at scales below 100 m to Langmuir circulations. A convergence over several tidal periods, as Fig. 13b and c show, is, however, counter-intuitive and puzzling. Reduced dispersion rates can possibly be understood in the light of the very regular appearance of the topography (and hence the related flow field) for the following reason: The 2D-kinematical equations, which relate particle trajectories to the Eulerian flow field, are nonlinear. The nonlinearity becomes manifest in that the individual trajectories *typically* behave in a chaotic way (i.e. mutual distances between particles increase exponentially in time). When a 'normal' dispersion coefficient (a coarse-grained averaged feature of this) is determined by these chaotic features of the flow, then an 'anomalously' low dispersion coefficient (possibly dropping to zero) must be related to the other well-known feature of such flows: the existence of trapping regions (Pasmanter [1988]). Another possibility is that such regions appear when the nonlinear kinematic equations become (near-) integrable (a feature which is absent in the general 2D-kinematical equations (Ottini et al. [1988]), and which is precisely the reason for the existence of chaotic trajectories). The strong regularity of the topography invokes the regularity of the flow field, making the kinematic equations integrable, the trajectories (near-) periodic, and thus the dispersion rate low.

Whether this qualitative argument is sufficient to explain observed low dispersion rates is still a subject of research. The existence of regions of unmixed fluid within a stirred environment has been found both numerically (Pasmanter [1988]) and in laboratory experiments (Ottini et al. [1988]). While the relevance of the mechanism of deterministic chaos to oceanic dispersion has been proposed by Zimmerman [1986], albeit for vigorous near-coastal areas only, most scientists hesitate to acknowledge that this is the *typical* way in which a 'normal' value of the dispersion coefficient is reached, while anomalous values of it derive from a degenerated system of kinematical equations. This is perhaps akin to the general, uncomfortable feeling which the study of dynamical systems first aroused, when establishing that all solvable classic text-book problems were *atypical* rather than generic.

6 Discussion

It is often required that Lagrangian information be derived from available Eulerian current information. The presented analysis indicates the feasibility of this under the strong provision that the bottom morphology, $H(\boldsymbol{x})$, is accurately known over the area of interest. This is required since variations in topography are 'translated' into Eulerian current fluctuations in two ways.

First, kinematically (~ $1/H$), at topographic length scales below the cross-isobath excursion scale U/σ, where U and σ denote the amplitude and frequency of the dominating current component. Second, dynamically (~ $1/H\ \nabla H$), at topographic scales of the same order as the cross-isobath excursion scale. The former process is uncomplicated and can, in principle, be tuned by a single current meter. The latter, however, reflects a (quasi-) nonlinear coupling of modes of motion, the magnitude of which can be estimated theoretically (Zimmerman [1978]), but whose actual impact is set by very local circumstances (the level of bottom friction, second-order interactions etc.) In practice, therefore, this requires additional Eulerian current information from other locations.

Current followers, such as drogues, sample the Eulerian current field successively at different positions. Thus spatial Eulerian current fluctuations introduce temporal Lagrangian current variations, a process which in the frequency domain shows up as spectral smearing of energy. Even though the energy in the Lagrangian spectrum is more distributed, this does not necessarily imply strong dispersion. It is observed that the level of the dispersion rate (the α in Section 5) is set by the presence, or absence, of chaos in the nonlinear kinematic equations, describing the trajectories of different particles. The kinematic equations of a 2D current system in general form a set of two nonlinearly coupled (non-integrable) equations, which allow for chaotic motions of the individual particles (i. e. distances between different particles increase exponentially in time). It is proposed that this nonlinear coupling is the *standard* situation, giving rise to relatively large dispersion rates (a bulk entity derived from it). In case of strong asymmetry in the topography, i. e. when the bottom is predominantly a function of *one* coordinate only, an effective *decoupling* of these equations occurs, leading to an *integrable* set of equations (such as the example in Section 4) and therefore to periodic trajectories and *trapping* of particles, characterized by low dispersion rates. Dispersion rates obtained from dye experiments, reported in the literature, do indicate the existence of a range of values α, both above and below 1. However, it will be interesting to check the conclusion arrived at in the present study (with strongly periodic topographies) against dispersion rates of drifters in areas with a random bottom, where nonlinear coupling does occur. It will then be required to focus on scales below the tidal excursion scale, as on such scales the shear dispersion by the residual current (which itself may be dynamically generated by the tide-topography interaction) produces enhanced dispersion rates.

Acknowledgements

The efforts and commitment demonstrated by R. Mulder and M. W. Manuels in acquiring the present data set are much appreciated. The moored current meter records were kindly provided by Rijkswaterstaat and H. W. Riepma of the Royal Netherlands Meteorological Institute. Discussions with J. M. Suijlen and comments on an earlier draft by J. T. F. Zimmerman were very helpfull.

This work was sponsored by the Netherlands Organization for Scientific Research (N. W. O).

References

Alphen, J. S. L. J. van and M. A. Damoiseaux, 1987: A morphological map of the Dutch shore face and adjacent continental shelf (1 : 250000) Internal report Rijkswaterstaat, directie Noordzee.

Attermeyer, M., 1974: Models for viscous dissipation of energy obtained from the Lagrangian form of the equations of motion. Phys. Fluids **17**, 679–687.

Bjerknes, V., J. Bjerknes, H. S. Solberg and T. Bergeron, 1933: Physikalische Hydrodynamik. Berlin: Springer, 787 pp.

Dietrich, G. and J. Ulrich, 1967: Atlas zur Ozeanographie. Mannheim: Meyers Gr. Phys. Weltatlas **7**, 1–75.

Kalkwijk, J. P. Th., 1986: Dispersion of matter at sea under homogeneous conditions, Dt. hydrogr. Z. **38**, 245–260.

Kawai, H., 1985: Scale dependence of divergence and vorticity of near-surface flows in the sea, Part I: Measurements and calculations of area-averaged divergence and vorticity. J. Oceanogr. Soc. Japan **41**, 157–166.

Longuet-Higgins, M. S., 1969: On the transport of mass by time-varying ocean currents. Deep-Sea Res. **16**, 431–447.

Molinari, R. and A. D. Kirwan, 1975: Calculation of differential kinematic properties of the Yucatan Current from Lagrangian observations. J. Phys. Oceanogr. **5**, 483–491.

Monin, A. S., 1962: On the Lagrangian equations of the hydrodynamics of an incompressible viscous fluid. Prikl. Mat. Mekh. **26**, 320–327 [J. Appl. Math. Mech. **26**, 458–465].

Mulder, R., 1982: Eulerian and Lagrangian analysis of velocity fields in the southern North Sea, **in** North Sea Dynamics, Sündermann/Lenz (eds.), Berlin-Heidelberg: Springer, 134–147.

Mulder, R. and M. W. Manuels, 1980: A description of drifter trajectories in the neighbourhood of current meters in the southern part of the North Sea near the coast of Texel. Internal report, Neth. Inst. Sea Res. Texel.

Mulder, R. and M. W. Manuels, 1982: Description of a drifter system used in experiments in the southern part of the North Sea. Dt. hydrogr. Z. **35**, 203–210.

Okubo, A., 1967: The effect of shear in an oscillatory current on horizontal diffusion from an instantaneous source. Int. J. Oceanol. Limnol. **1**, 194–204.

Okubo, A. and C. C. Ebbesmeyer, 1976: Determination of vorticity, divergence and deformation rates from analysis of droque observations. Deep-Sea Res. **23**, 349–352.

Okubo, A., C. C. Ebbesmeyer, J. M. Helseth and A. S. Robbins, 1976: Reanalysis of the Great Lakes drogue studies data. Final report. Special report Mar. Sc. Res. Center.

Ottini, J. M., C. W. Leong, M. Rising and P. D. Swanson, 1988: Morphological structures produced by mixing in chaotic flows. Nature **333**, 419–425.

Ozmidov, R. V., 1965: Energy distribution between oceanic motions of different scales. Izv. Atm. Ocean Phys. **1**, 257–261.

Pasmanter, R. A., 1988: Anomalous diffusion and anomalous stretching in vortical flows. Fluid Dyn. Res. **3**, 320–326.

Pierson, W. J., jr, 1962: Perturbation analyis of the Navier-Stokes equations in Lagrangian form with selected linear solutions. J. Geoph. Res. **67**, 3151–3160.

Ramster, J. W. and J. A. Durance, 1975: Stokes' drift and the sacred-cow syndrome. ICES Hydrography Committee CM. 1975/C:14, 1–9 (unpublished document).

Riepma, H. W., 1987: Topographically induced tidal vorticity in a shallow homogeneous sea area. Oceanologica Acta **10**, 393–401.

Robinson, I. S., 1983: Tidally induced residual flow. **In**: Physical Oceanography of Coastal and Shelf Seas, Johns, B. (ed.), Elsevier, 321–357.

Sanderson, B. G., 1985: A Lagrangian solution for internal waves. J. Fluid Mech. **152**, 191–202.

Sanderson, B. G. and A. Okubo, 1986: An analytical calculation of two-dimensional dispersion. J. Oceanogr. Soc. Japan **42**, 139–153.

Suijlen, J. M., J. S. Sydow, C. Heins and P. C. Beukenkamp, 1990: Meting van turbulente diffusie en reststromen in de Zuidelijke Noordzee met merkstof experimenten in 1982. Rijkswaterstaat, Tidal Waters Division. Report in preparation.

Taylor, G. I., 1953: Dispersion of soluble matter in solvent flowing slowly through a tube. Proc. Roy. Soc. (A) **219**, 186–203.

Watson, G. N., 1966: Theory of Bessel functions. Cambridge University Press, 804 pp.

Young, W. R., P. B. Rhines and C. J. R. Garrett, 1982: Shear-flow dispersion, internal waves and horizontal mixing in the Ocean. J. Phys. Oceanogr. **12**, 515–527.

Zimmerman, J. T. F., 1978: Topographic generation of residual circulation by oscillatory (tidal) currents. Geoph. Astroph. Fluid Dyn. **11**, 35–47.

Zimmerman, J. T. F., 1979: On the Euler-Lagrange transformation and the Stokes' drift in the presence of oscillatory and residual currents. Deep-Sea Res. **26A**, 505–520.

Zimmerman, J. T. F., 1986: The tidal whirlpool: a review of horizontal dispersion by tidal and residual currents. Neth. J. Sea Res. **20**, 133–154.

Eingegangen am 6. Juni 1989

Angenommen am 16. November 1989

Anschrift des Verfassers:

Leo R. M. Maas

Netherlands Institute for Oceanic Sciences, P. O. Box 59, 1790 AB Den Burg, Texel, Niederlande